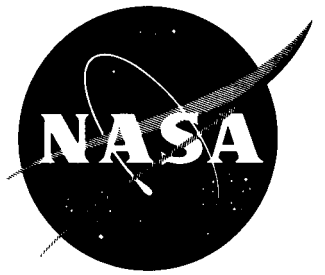

TECHNICAL NOTE

D-1784

AN EXPERIMENTAL INVESTIGATION OF THE EFFECTIVENESS OF SINGLE ALUMINUM METEOROID BUMPERS

By Donald H. Humes

Langley Research Center
Langley Station, Hampton, Va.

NATIONAL AERONAUTICS AND SPACE ADMINISTRATION

WASHINGTON May 1963

NATIONAL AERONAUTICS AND SPACE ADMINISTRATION

TECHNICAL NOTE D-1784

AN EXPERIMENTAL INVESTIGATION OF THE EFFECTIVENESS OF SINGLE ALUMINUM METEOROID BUMPERS

By Donald H. Humes

SUMMARY

An experimental investigation of the effectiveness of single aluminum meteoroid bumpers has been made. For impact velocities up to 15,000 ft/sec, the penetration of 0.062-inch-diameter copper spheres into aluminum targets can be greatly reduced by using a properly selected bumper placed an adequate distance from the main wall. In the velocity range of this investigation, there was a limit to the depth to which some bumper-protected targets were penetrated that occurred at a relatively low impact velocity, the lower velocity projectiles producing deeper penetrations than the higher velocity projectiles. The effectiveness of the bumper against the higher velocity projectiles was caused by the shattering of the projectiles as they penetrated the bumper at these velocities and by the dispersion of the resulting fragments over a large area of the main wall. The degree of fragmentation was a function of the impact velocity.

The limit to which the aluminum bumper-protected targets were penetrated by copper spheres is a function of the bumper thickness. The optimum bumper thickness was between 0.5 and 2.0 times the diameter of the impacting projectile. At velocities great enough to cause fragmentation of the projectile, the penetration decreased with increased bumper standoff distance, up to a point, beyond which further increases in the bumper standoff distance had no effect on the penetration. A standoff distance greater than 8 projectile diameters was required to limit penetration in a bumper-protected target.

INTRODUCTION

Meteoroids pose a potential hazard to space vehicles. Considerable research is being directed to define this hazard. If it is discovered that the meteoroid hazard is great, a means of reducing the hazard must be found. Several fabrication techniques to reduce the damage from meteoroid impact are currently being studied. This report describes an investigation of a meteoroid bumper, which is a concept first proposed by Whipple as a means of reducing impact damage. (See ref. 1.)

A meteoroid bumper is a thin shield placed a short distance from the main wall of a space vehicle. Whipple envisioned that meteoroids would be fragmented

or even vaporized while penetrating the bumper and that the resulting debris or vapor would be dispersed over a large area of the main wall. This fragmentation and dispersion would result in reduced penetration at any one point.

This investigation was conducted to determine whether projectiles traveling in the velocity range from 0 to 15,000 ft/sec could be shattered while penetrating a meteoroid bumper, to determine whether meteoroid bumpers could reduce the penetration into targets by such projectiles, and also to determine the effect of bumper thickness and standoff distance on bumper effectiveness. Impact data were obtained for bumpers varying in thickness from 0.010 inch to 0.250 inch to determine their effectiveness in reducing the penetration of 0.062-inch-diameter copper spheres. The bumper standoff distance was varied from 0 to 6 inches. Aluminum spheres 0.22 inch in diameter were used as projectiles in the photographic studies conducted to determine whether shattering occurred.

SYMBOLS

d	projectile diameter
h	standoff distance
P	total penetration depth
P_{max}	maximum total penetration depth for projectiles traveling in the velocity range from 0 to 15,000 ft/sec
P_{mw}	deepest penetration in main wall of a bumper-protected target
t_B	bumper thickness

APPARATUS AND TEST TECHNIQUE

Projectiles and Targets

The bumper-protected targets tested in this investigation consisted of a quasi-infinite main wall of 2024-T4 aluminum alloy and a single bumper of 2024-T3 or 2024-T4 aluminum alloy separated by a short distance. The two alloys were used interchangeably to take advantage of available material. The two alloys should behave practically the same because of the similarity in their mechanical properties. A comparison of the mechanical properties of 2024-T3 and 2024-T4 aluminum alloys as obtained from reference 2 is as follows:

	2024-T3	2024-T4
Modulus of elasticity, psi	10.6×10^6	10.6×10^6
Brinell hardness	120	120
Ultimate tensile strength, psi	70,000	68,000
Yield tensile strength, psi	50,000	47,000
Shearing strength, psi	41,000	41,000
Elongation (in 2 in.) of 1/16-inch specimen, percent	18	20

A sketch defining the bumper-protected target arrangement and a photograph of the actual type used are shown in figure 1.

Bumper thickness was varied from 0.010 inch to 0.250 inch and the standoff distance was varied from 0 to 6 inches.

The projectiles were 0.062-inch-diameter spheres made of electrolytic tough pitch copper and 0.220-inch-diameter spheres made of 2024-T4 aluminum alloy. The copper spheres were used in the impact tests so that projectile material remaining in a crater could be easily detected.

Projectile Launching Technique

A 220 Swift rifle was used to accelerate the projectiles to velocities up to 7,000 ft/sec. In order to obtain greater velocities, the projectiles were accelerated in a helium light-gas gun with a 0.220-inch-diameter launch tube bore. A description of this gun can be found in reference 3.

Each 0.062-inch-diameter sphere was mounted on a cylindrical magnesium sabot, 0.220 inch in diameter and 0.110 inch long. When the sabot left the launch tube, its edge struck a steel bar deflector. The small spherical projectile continued along the flight path while the sabot was deflected and hence separated from the projectiles. The 0.220-inch-diameter aluminum spheres were launched from the 22-caliber launch tubes without the use of sabots.

Velocity Measuring Technique

The velocity of the projectiles was determined by placing two sheets of Mylar, aluminized on both sides, along the flight path at a known distance apart. The separation distance was 1 foot for the impact tests and 7 feet when the impact photographs were taken. The total thickness of the Mylar insulator and the aluminum coatings was 0.00025 inch. A potential was applied between the aluminum coatings on each Mylar sheet. When the projectile penetrated the first sheet, the aluminum was ionized by the impact and momentarily formed a conducting path between the two aluminum surfaces. The resulting discharge started an electronic time-interval counter. A similar pulse from the second sheet stopped the counter. The impact velocity was considered equal to the velocity measured by this technique.

Penetration Measuring Technique

Penetrations into the bumpers that were not completely penetrated and into the main walls were measured from the original surface of the undisturbed material to the deepest point in the crater. The penetration into a completely penetrated bumper was considered equal to the bumper thickness. The total penetration was the sum of the penetration into the bumper and the penetration into the main wall. Penetration depths were measured with a depth gage which was tapered from a 0.031-inch-diameter stem to a 0.005-inch-diameter point over a 0.106-inch length.

Photographing Technique

The photographs of projectiles penetrating the bumpers were taken with a high-speed framing camera at the rate of approximately 600,000 frames per second. A schematic diagram of the arrangement of the apparatus used to obtain the impact photographs is illustrated in figure 2. The camera was placed at one window in the test chamber. A xenon tube, used as a high-intensity short-duration light source, was placed outside a second window directly across from the first. A Fresnel lens placed over the second window focused the light through the camera lens. The camera shutter was open for the entire test but the film was exposed only while the xenon tube emitted light. The time delay as measured between the Mylar sheets was used to trigger the light source as the projectile passed by the window.

PRESENTATION OF RESULTS

The ability of a bumper to reduce penetration depends on its ability to shatter impacting projectiles and to disperse the resulting debris over a large area of the main wall. In order to determine if projectile fragmentation and dispersion would occur, photographs of 0.220-inch-diameter 2024-T4 aluminum-alloy spheres as they penetrated 0.125-inch-thick 2024-T3 aluminum-alloy bumpers were taken at various impact velocities with a high-speed framing camera. The photographs in figure 3 show the projectile and bumper fragments shortly after the bumpers had been penetrated. The bumper is the vertical line extending from the top to the bottom of the photograph. The two short vertical lines are reference marks placed 1 inch apart and are out of the flight path of the projectiles. The projectiles were moving from left to right.

A projectile which impacted the bumper at 2,780 ft/sec passed through the bumper intact and essentially undeformed, as shown in figure 3(a). The projectile is the leading particle and a plug punched from the bumper follows behind. A ring of bumper material can be seen being spalled from the exit side of the bumper. An impact velocity of 4,850 ft/sec caused both the projectile and the bumper plug to be shattered; however, the projectile fragments remained clustered at the leading edge of the fragment field, as shown in figure 3(b). At an impact velocity of 7,250 ft/sec, the projectile was shattered and the fragments were dispersed. The projectile fragments are indistinguishable from the bumper fragments. (See fig. 3(c).) The impact velocity of 13,400 ft/sec caused much greater fragmentation and dispersion. The individual fragments were small in comparison with the original projectile size. (See fig. 3(d).) A sequence of photographs of the dispersion of fragments which took place after this particular impact is shown in figure 4.

The damage which the fragments of a shattered projectile would cause to a main wall depends on their individual size and velocity and also on the number which strike the main wall within the bounds of a crater caused by a faster fragment, resulting in a deeper compound crater.

The photographs in figure 3 and similar photographs at different impact velocities show that the number of fragments increased and their size decreased with increasing impact velocity.

The manner in which the fragments were dispersed (see fig. 4) indicates that the number of compound craters depends on the standoff distance. A short standoff distance would result in a concentration of fragments on a small area of the main wall. A larger standoff distance would result in a dispersion of fragments over a larger area and hence fewer compound craters.

The velocity of the fragments was obtained from sequence photographs similar to those shown in figure 4. The velocity of the individual fragments created by any one impact varied greatly, with those at the leading edge of the fragment field possessing the maximum velocity. The maximum fragment velocity is shown as a function of the impact velocity in figure 5. In this figure, the bumpers were 0.125 inch thick and the aluminum projectiles had diameters of 0.220 inch. The maximum fragment velocity was always less than the impact velocity. As the impact velocity was increased the maximum fragment velocity increased.

The photographic study shows that at high impact velocities the projectiles were shattered by the bumper into many small particles; each fragment possessed only a small fraction of the initial kinetic energy of the projectile. The photographs also show that the particles are well dispersed so that the residual energy will be used in producing many small craters rather than a single deep crater. The depth of these craters cannot be accurately predicted from the photographs because of the inability to define accurately the size and material of the fragments and the number of compound craters that will occur. The actual effectiveness of the bumpers was determined from penetration data obtained in additional tests. (See tables I and II.)

Penetration Data

Impact velocity.- The effectiveness of a bumper was determined by comparing the total penetration in the bumper system (which is the penetration into the bumper plus the penetration into the main wall) with the penetration into a quasi-infinite target under the same impact conditions. The penetration of copper spheres into quasi-infinite targets and bumper-protected targets is shown in figure 6. The penetration into the quasi-infinite target increased with increasing impact velocity for the entire velocity range.

The total penetration into the bumper-protected target increased as the impact velocity increased in the low-velocity range. At 10,000 ft/sec (see fig. 6), the penetration reached a maximum value and decreased with further increases in the impact velocity. The bumper thickness was 0.5 the projectile diameter and the standoff distance was 32 projectile diameters.

At velocities up to 8,000 ft/sec, the bumper did not reduce the penetration. In fact, the total penetration was greater than that in the unprotected target. In this velocity range, the copper projectiles remained intact after penetrating the bumper. A crater formed in the main wall by an intact, unfragmented projectile is shown in figure 7(a), which is a photograph of the bumper and main wall

of the target impacted at 6,350 ft/sec. The increased penetration in this velocity range was a result of the finite thickness of the bumper. According to reference 4, less momentum is required to penetrate a finite plate than is required to penetrate a quasi-infinite plate to a depth equal to the plate thickness. Therefore, a projectile which remains intact after penetrating a bumper has more momentum left than a projectile which has penetrated the same depth of material in a quasi-infinite target.

At velocities above 8,000 ft/sec, the projectiles were shattered and the bumper was effective in reducing penetration. The maximum penetration which this bumper-protected target received was caused by a projectile traveling 9,950 ft/sec At this velocity the projectile was shattered; however, the fragments remained clustered and formed a deep, irregular, compound crater. (See fig. 7(b).) As the impact velocity increased above 10,000 ft/sec, the fragmentation and dispersion of fragments became more complete. In figure 7(c) are shown the bumper and main wall of the target impacted at 12,860 ft/sec. At this impact velocity the projectile was shattered and the fragments dispersed to form many individual craters.

As previously mentioned, the penetration resulting from fragments of a shattered projectile depends on the size and velocity of the fragments as well as on the cumulative effect of compound cratering. Examination of the craters in the main walls showed that the number of fragments increased as the impact velocity increased. This conclusion is in agreement with the impact photographs taken of aluminum projectiles. The impact photographs also showed that the velocity of the fragments increased with increased impact velocity. The decrease in penetration in the bumper-protected target in the high-velocity range indicates that the increase in fragmentation and dispersion had a greater influence on the penetrating ability of the fragments than did the increase in fragment velocity.

Bumper standoff distance.- The effect of the standoff distance on the total penetration of copper spheres was determined by impacting bumper-protected targets at various standoff distances while holding the bumper thickness and impact velocity constant. The particular bumper used had a thickness equal to 0.5 the projectile diameter - that is, 0.031 inch. The results of this study are shown in figure 8.

At impact velocities below 9,000 ft/sec, the penetration was independent of the bumper standoff distance as illustrated by the data curves at 2,000 and 9,000 ft/sec. At these velocities the projectile remained essentially intact. At velocities greater than 9,000 ft/sec, the penetration decreased as the standoff distance increased, up to a point, beyond which further increases in the standoff distance had no effect on the penetration, as witnessed by the data curves at 10,000, 12,000, and 14,000 ft/sec. At impact velocities greater than 9,000 ft/sec the projectile was shattered. Increasing the standoff distance resulted in a reduction of compound cratering and hence a reduction in penetration. When the standoff distance was great enough for virtually eliminating compound cratering, further increases in the standoff distance had no effect on the penetration.

A standoff distance of approximately 50 times the projectile diameter was required to take full advantage of the dispersion of fragments when the impact velocity was 12,000 ft/sec. A standoff distance greater than 8 projectile diameters is required to cause the total penetration to decrease with increasing

impact velocities from 9,000 ft/sec to 14,000 ft/sec. However, the maximum depth to which this bumper-protected target was penetrated was constant for all standoff distances greater than 8 projectile diameters. The maximum penetration of 2.4 times the projectile diameter was produced by projectiles traveling 9,000 ft/sec. For standoff distances less than 8 projectile diameters, an increase in the impact velocity always resulted in increased penetration.

Bumper thickness.- Six bumper-protected targets varying only in the thickness of the bumper were tested at various velocities to determine which bumper was the most effective in reducing the penetration of copper projectiles. The penetration-velocity curves for these six bumper-protected targets are shown in figure 9. The standoff distance was 16 times the projectile diameter, and the bumper thickness was varied from 0.16 to 4.0 times the projectile diameter. The long-dashed line in each part of figure 9 shows the total penetration required to penetrate the bumper itself. The short-dashed curve is the penetration into an unprotected quasi-infinite target and is the experimentally determined curve previously shown in figure 6.

The thin bumpers, 0.16 and 0.25 projectile diameters thick, shown in figures 9(a) and 9(b), respectively, caused the projectile to shatter at impact velocities greater than 10,000 ft/sec. At velocities above 10,000 ft/sec the bumper was effective in reducing the penetration slightly. The projectiles were not shattered to the degree necessary to produce both a maximum penetration and a subsequent continuous decrease in penetration as seen in figure 6.

The thicker bumpers, 0.5 and 1.0 projectile diameters thick, shown in figures 9(c) and 9(d), respectively, did cause fragmentation sufficient to produce a maximum and subsequent decrease in penetration. Hence, these bumpers were very effective in reducing penetration at velocities greater than 9,000 ft/sec.

The penetration into the bumper-protected target that had a bumper thickness of 2.0 projectile diameters appears to have reached a maximum value at 10,000 ft/sec; however, a subsequent decrease in penetration is not evident. (See fig. 9(e).) In this case most of the penetration was into the bumper itself. This bumper was effective in reducing penetration at velocities above 10,000 ft/sec.

The bumper which was 4.0 projectile diameters thick was excessive. (See fig. 9(f).) The penetration of 4.0 projectile diameters required to penetrate the bumper itself is greater than the maximum total penetrations into the targets having thinner bumpers. This bumper was ineffective at all test velocities.

A comparison of the effectiveness of these six bumpers can be made by comparing the percent reduction in total penetration at any given velocity or by comparing the maximum depth to which each was penetrated in the velocity range of this investigation. The latter method, which is more meaningful when the impact velocity is unknown, was chosen.

The maximum penetrations of copper spheres obtained in the velocity range from 0 to 15,000 ft/sec are shown in figure 10 as a function of the bumper thickness. The long-dashed line represents total maximum penetration equal to bumper thickness. The spread at bumper thicknesses of 0.5 and 1.0 projectile diameters

shows the degree to which data were scattered in the velocity range in which the maximum penetration occurred. The circular data point for the bumper thickness of 2.0 projectile diameters indicates a well-defined value of maximum penetration. However, this maximum was determined from only a few data points which happened to provide a smooth curve. The arrows indicate the bumper systems which had no peak penetration in the velocity range of this investigation. The base of the arrow is located at the deepest penetration obtained in this investigation.

The maximum penetration is definitely a function of bumper thickness. The maximum penetration into bumper-protected targets that had bumper thicknesses between 0.5 and 2.0 projectile diameters was less than the penetrations observed in targets which had either thicker or thinner bumpers. The bumper-protected target that had a bumper thickness of 0.5 projectile diameter was the most effective in reducing penetration damage.

DISCUSSION

Meteoroids approach the earth from all directions and with a wide range of speeds. In some cases the velocities of a meteoroid and a space vehicle in the vicinity will be subtractive and a low, nearly zero, impact velocity will result. In other cases the velocities will be additive and an impact velocity of over 200,000 ft/sec will result. The data contained in this report were obtained in only a small portion of the range of expected impact velocities between meteoroid and space vehicle. The trends observed in this investigation are clear; however, any extrapolation to meteoric velocities should be done with care.

If the trends observed in the velocity range from 0 to 14,000 ft/sec for the bumper-protected target in figure 6 persist at velocities greater than 14,000 ft/sec, then the penetration depth will continue to decrease with increasing impact velocity, until at some velocity the fragmentation and dispersion may be so complete that only negligible penetration damage is inflicted to a very thick main wall. If this is the case, then the maximum penetration observed at 10,000 ft/sec would be the absolute maximum penetration obtained in the velocity range from 0 to 200,000 ft/sec. The optimum bumper thickness of 0.5 to 2.0 projectile diameters, as obtained from the present tests, would not only be applicable to the range from 0 to 14,000 ft/sec, but for the full range of meteoroid impact velocities provided that the main wall is quasi-infinite.

In order to convert the data to finite-thickness main walls expected in space vehicles, the total finite thickness of aluminum required to prevent particle penetration was calculated by multiplying the maximum penetration into the main wall by a factor of 1.5 and adding this to the bumper thickness. It has been shown in reference 4 that a finite plate will just prevent complete penetration of a projectile if the plate thickness is 1.5 times the depth the particle would have penetrated in a quasi-infinite plate. The results of the calculations are shown in figure 11. The curve shows that a minimum total thickness of approximately 3 projectile diameters will prevent particle penetration for all the copper projectiles traveling in the velocity range from 0 to 15,000 ft/sec provided that the bumper thickness is between 0.5 and 2.0 projectile diameters. This thickness

may be capable of preventing particle penetration through the full range of meteoroid velocities.

The use of a finite-thickness main wall makes other considerations necessary. Besides penetration damage from individual fragments, a thin finite main wall may fail because of the pressure pulse created when the many projectile and bumper fragments strike the main wall. This type of damage may possibly be eliminated by using a large standoff distance, possibly many times that required to limit particle penetration.

The shape of the curve in figure 10 is believed to be representative and will occur when other projectiles and bumpers are tested. However, the magnitude of the maximum penetration and the optimum bumper thickness will probably vary with projectile and bumper materials.

CONCLUSIONS

The results of this experimental investigation of the effectiveness of single aluminum meteoroid bumpers have shown that -

1. At high impact velocities the projectiles were shattered by the bumper into many small particles, each of which possessed only a small fraction of the initial kinetic energy of the projectile.

2. In some bumper-protected targets the penetration increased as the impact velocity increased until a maximum total penetration was reached at approximately 10,000 ft/sec. The total penetration decreased with further increases in the impact velocity.

3. At velocities too low to cause fragmentation of the projectile, the total penetration is independent of bumper standoff distance.

4. At velocities great enough to cause projectile fragmentation, the total penetration decreased with increased bumper standoff distance, up to a point, beyond which further increases in bumper standoff distance had no effect on the total penetration.

5. A standoff distance greater than 8 projectile diameters is required to cause the total penetration to decrease with increasing impact velocities from 9,000 ft/sec to 14,000 ft/sec.

6. The maximum total penetration observed in a bumper-protected target in the velocity range from 0 to 15,000 ft/sec was definitely a function of the bumper thickness. The bumper thickness of 0.5 the projectile diameter produced the lowest maximum total penetration and is therefore considered the most effective bumper thickness of those investigated.

Any attempt to predict the behavior of bumper-protected targets when impacted by meteoroids with the use of the data contained in this report should be

done with care. If meteoroids can be shattered by bumpers to the same degree that the copper and aluminum spheres were, meteoroid bumpers could be very effective against high-velocity meteoroids.

Langley Research Center,
National Aeronautics and Space Administration,
Langley Station, Hampton, Va., February 11, 1963.

REFERENCES

1. Whipple, Fred L.: Meteoritic Phenomena and Meteorites. Physics and Medicine of the Upper Atmosphere, Clayton S. White and Otis O. Benson, Jr., eds., The Univ. of New Mexico Press (Albuquerque), 1952, pp. 137-170.

2. Anon.: Alcoa Aluminum Handbook. Aluminum Co. of America, c.1957, p. 20.

3. Collins, Rufus D., Jr., and Kinard, William H.: The Dependency of Penetration on the Momentum Per Unit Area of the Impacting Projectile and the Resistance of Materials to Penetration. NASA TN D-238, 1960.

4. Kinard, William H., Lambert, C. H., Jr., Schryer, David R., and Casey, Francis W., Jr.: Effect of Target Thickness on Cratering and Penetration of Projectiles Impacting at Velocities to 13,000 Feet Per Second. NASA MEMO 10-18-58L, 1958.

TABLE I.- IMPACT DATA FOR 0.062-INCH-DIAMETER COPPER SPHERES STRIKING QUASI-INFINITE ALUMINUM TARGETS

Impact velocity, ft/sec	Penetration, in.
1,700	0.032
2,450	.055
3,400	.085
4,100	.098
5,380	.107
6,030	.120
6,850	.133
8,040	.139
10,690	.182
10,790	.184
10,860	.185
11,950	.182
13,140	.187

TABLE II.- IMPACT DATA FOR 0.062-INCH-DIAMETER COPPER SPHERES STRIKING QUASI-INFINITE ALUMINUM TARGETS

PROTECTED BY SINGLE ALUMINUM BUMPERS

Impact velocity, ft/sec	Total penetration, in.
t_B = 0.031 in.; h = 2 in.	
2,080	0.068
3,080	.089
3,860	.112
5,600	.139
6,350	.140
6,780	.136
7,480	.140
9,050	.150
9,430	.146
9,840	.134
9,950	.154
11,170	.110
11,800	.123
12,310	.120
12,860	.110
14,040	.091
t_B = 0.010 in.; h = 1 in.	
1,610	0.036
2,660	.066
3,080	.080
3,870	.094
4,360	.099
5,520	.114
6,460	.129
6,920	.135
8,310	.146
9,170	.164
11,230	.189
12,500	.164
t_B = 0.016 in.; h = 1 in.	
2,620	0.068
3,640	.095
4,850	.107
5,760	.127
6,420	.129
7,120	.136
8,020	.158
8,850	.158
9,350	.166
10,000	.177
10,300	.148
10,990	.138
11,710	.141
14,550	.158
15,500	.169
t_B = 0.031 in.; h = 1 in.	
2,200	0.070
2,220	.087
2,520	.097
3,400	.113
5,060	.115
5,500	.124
5,800	.133
6,240	.144
6,600	.128
7,120	.139
8,390	.130
9,825	.139
10,400	.125
12,050	.125
12,150	.118
14,960	.103

Impact velocity, ft/sec	Total penetration, in.
t_B = 0.062 in.; h = 1 in.	
1,540	0.033
2,590	.109
3,590	.120
4,510	.117
5,490	.116
5,750	.128
6,300	.133
6,670	.134
7,440	.130
7,860	.158
7,870	.132
8,720	.169
8,810	.138
9,010	.155
9,950	.146
10,520	.125
12,000	.128
12,450	.122
t_B = 0.125 in.; h = 1 in.	
1,580	0.043
4,500	.140
5,100	.139
5,640	.149
6,050	.141
6,500	.137
7,030	.144
7,580	.148
7,930	.153
9,590	.173
10,910	.166
11,280	.164
12,320	.163
t_B = 0.250 in.; h = 1 in.	
1,850	0.034
2,580	.056
3,470	.091
5,380	.110
5,950	.122
6,350	.153
7,660	.158
8,050	.164
12,210	.238
t_B = 0.031 in.; h = 0 in.	
9,430	0.144
9,710	.156
12,280	.178
14,280	.182
t_B = 0.031 in.; h = 4 in.	
2,280	0.062
9,620	.137
12,500	.102
t_B = 0.030 in.; h = 6 in.	
2,050	0.056
9,350	.147
9,900	.142
12,150	.101

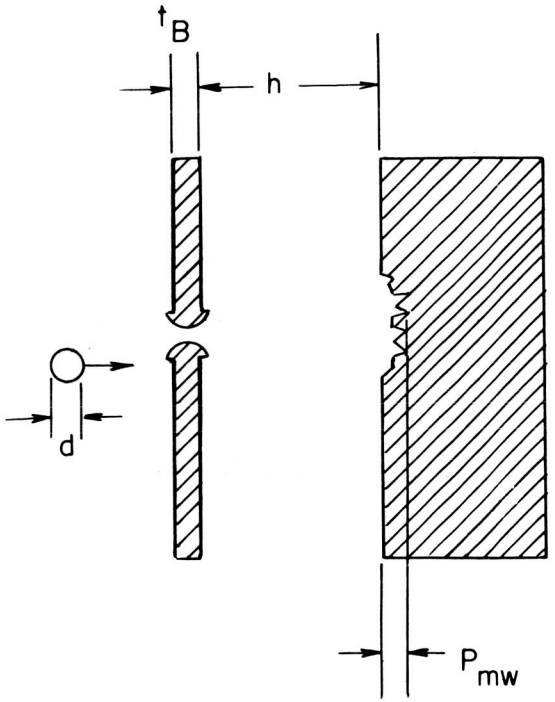

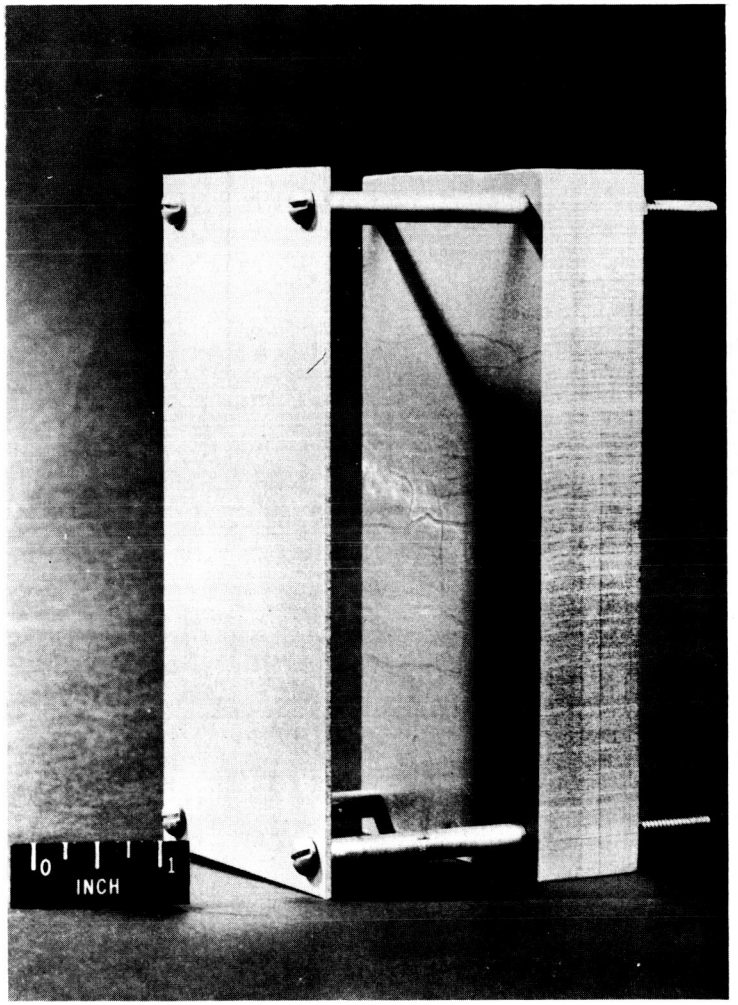

Figure 1.- Bumper-protected target configuration. L-62-252

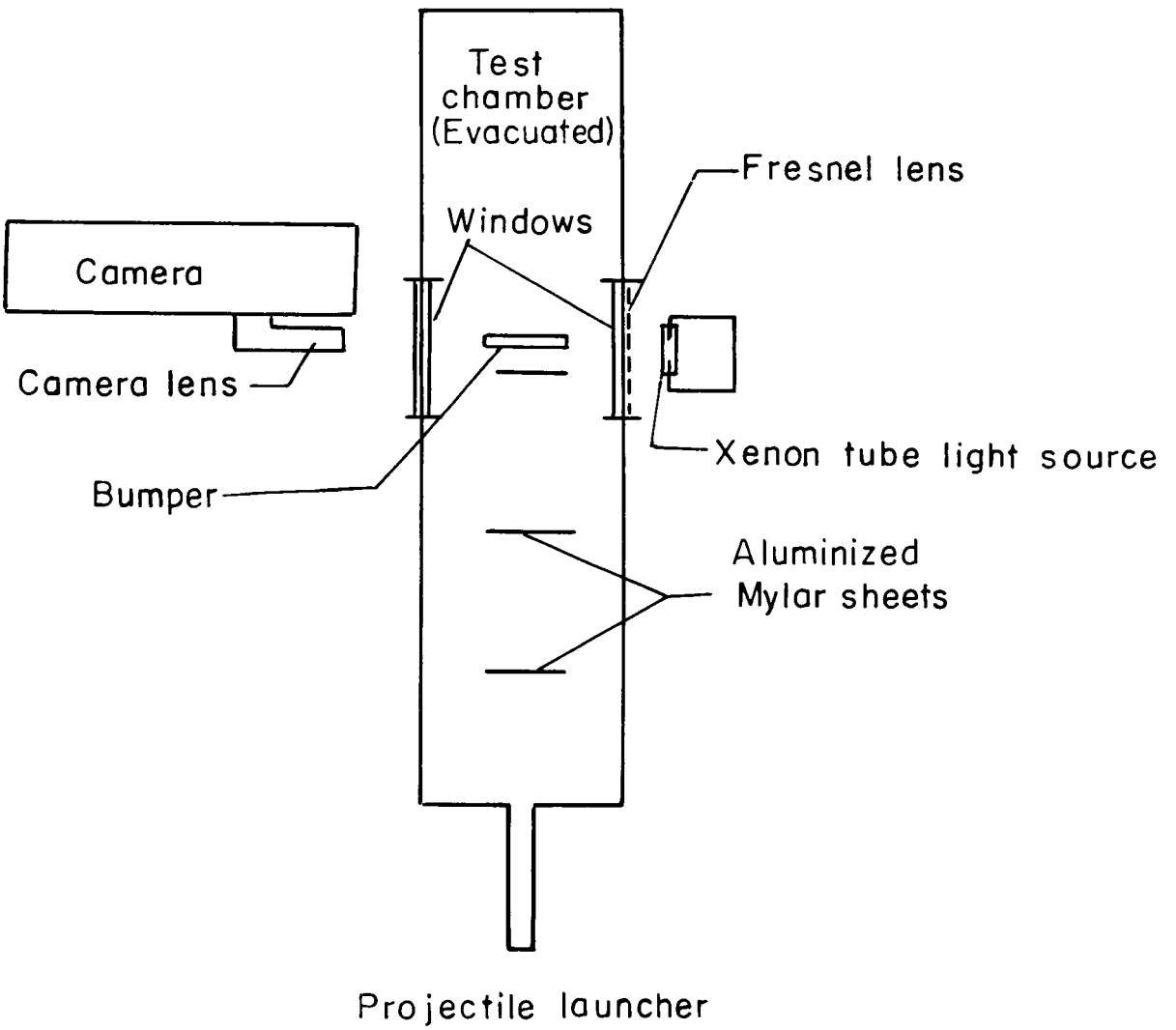

Figure 2.- Apparatus used in photographing technique.

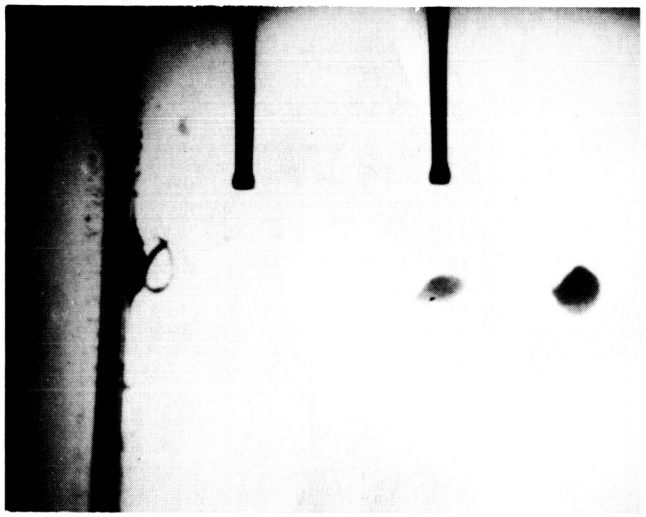

(a) 2,780 ft/sec.

(b) 4,850 ft/sec.

(c) 7,250 ft/sec.

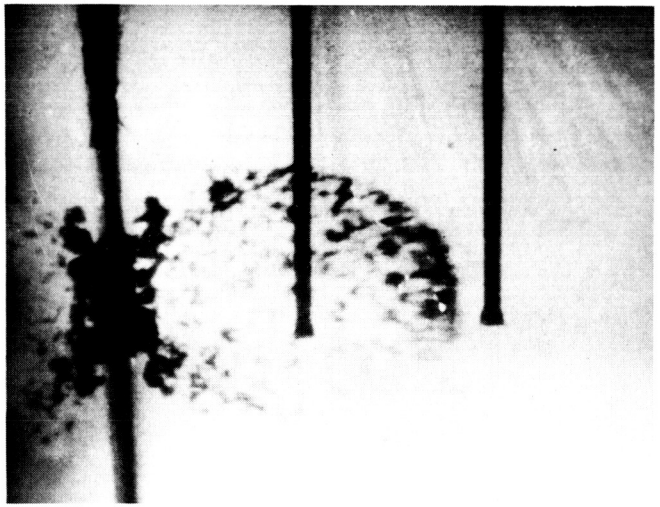

(d) 13,400 ft/sec.

L-61-5071

Figure 3.- Projectile fragmentation by bumpers at various impact velocities. Bumpers were 0.125-inch-thick 2024-T3 aluminum alloy; projectiles were 0.220-inch-diameter 2024-T4 aluminum-alloy spheres.

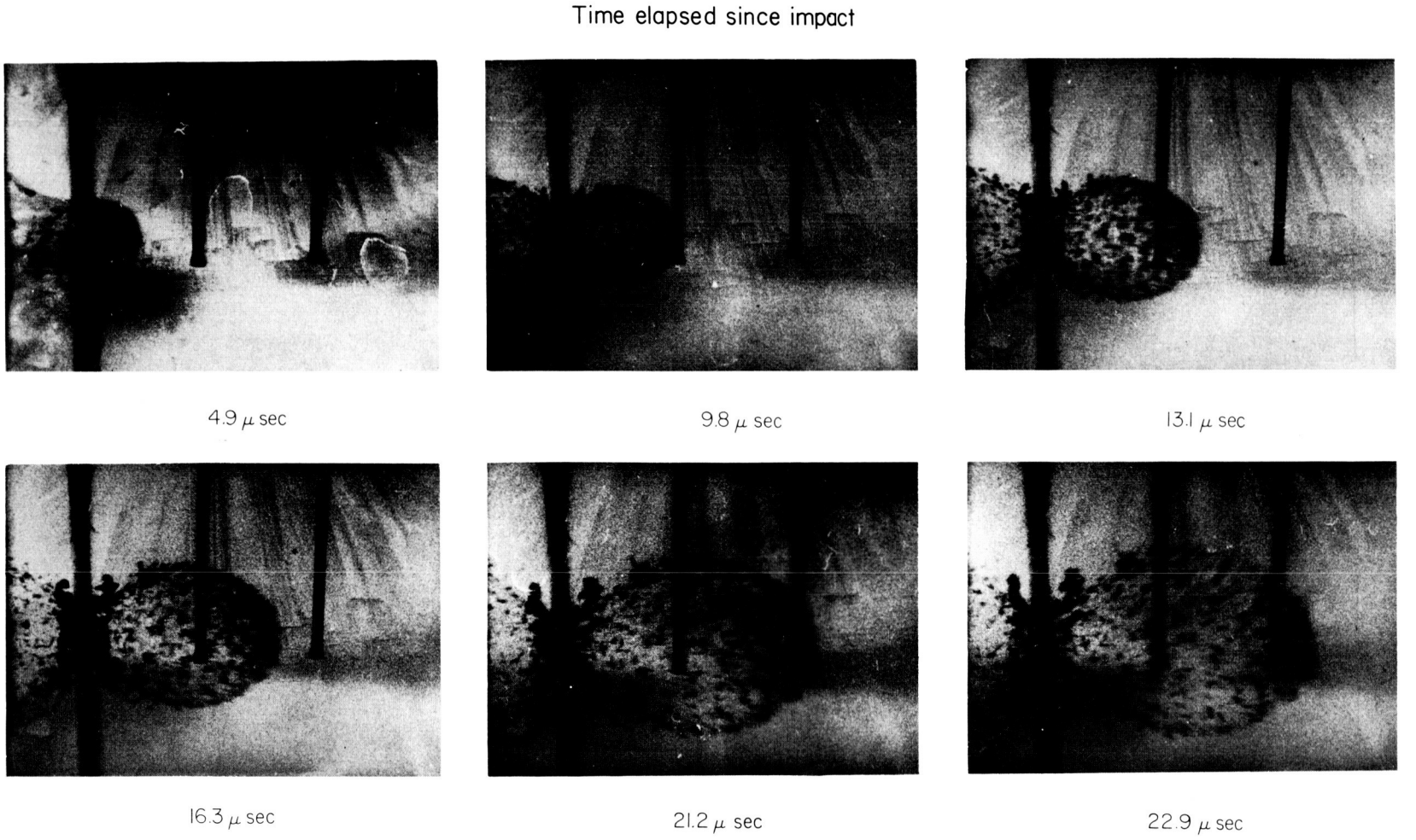

L-63-58

Figure 4.- Dispersion of fragments after impact on bumper shield. Bumper was 0.125-inch-thick 2024-T3 aluminum alloy; projectile was a 0.220-inch-diameter sphere of 2024-T4 aluminum alloy; impact velocity = 13,400 ft/sec.

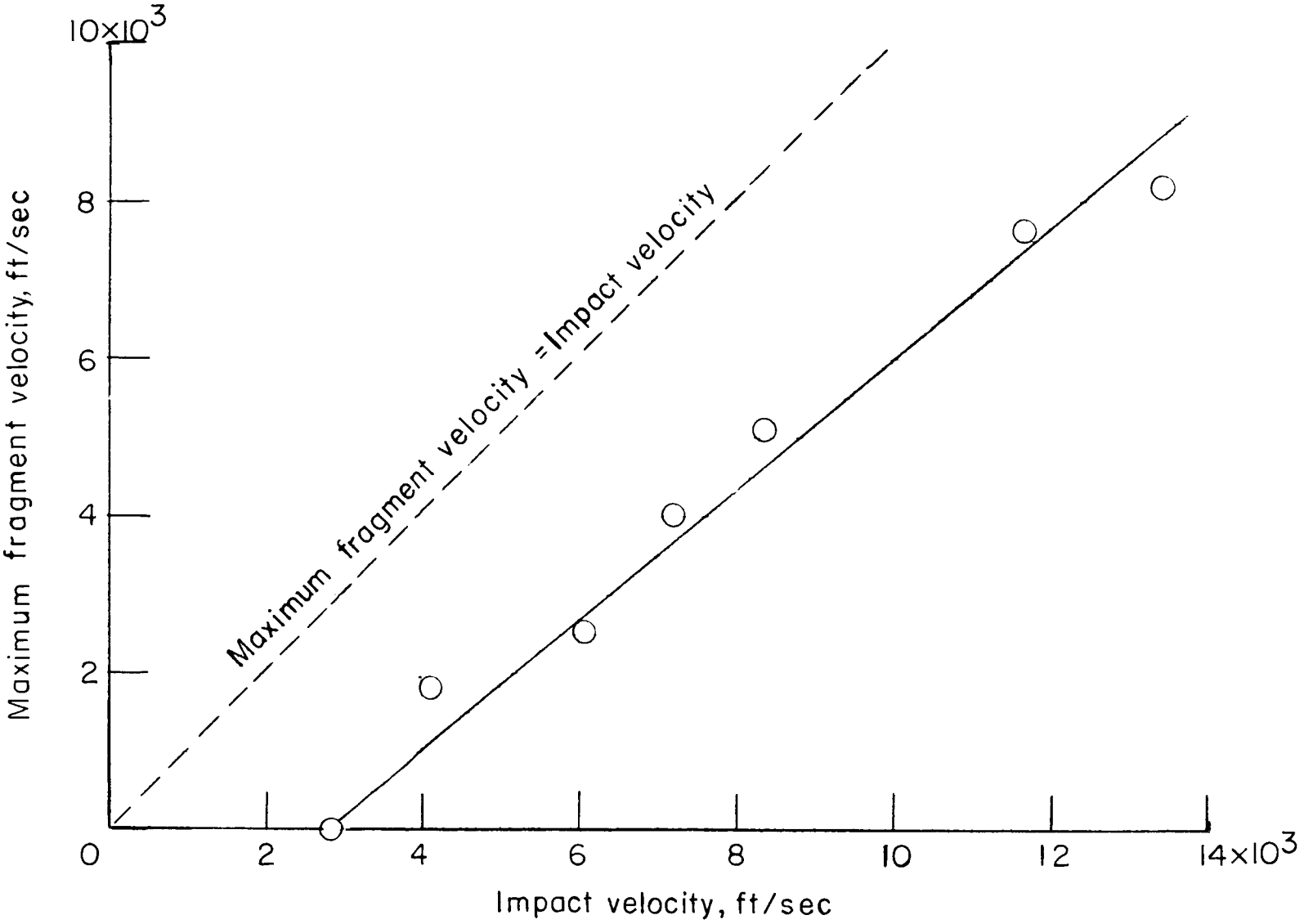

Figure 5.- Maximum fragment velocities observed at various projectile impact velocities. Bumpers were 0.125-inch-thick 2024-T3 aluminum alloy; projectiles were 0.220-inch-diameter 2024-T4 aluminum-alloy spheres.

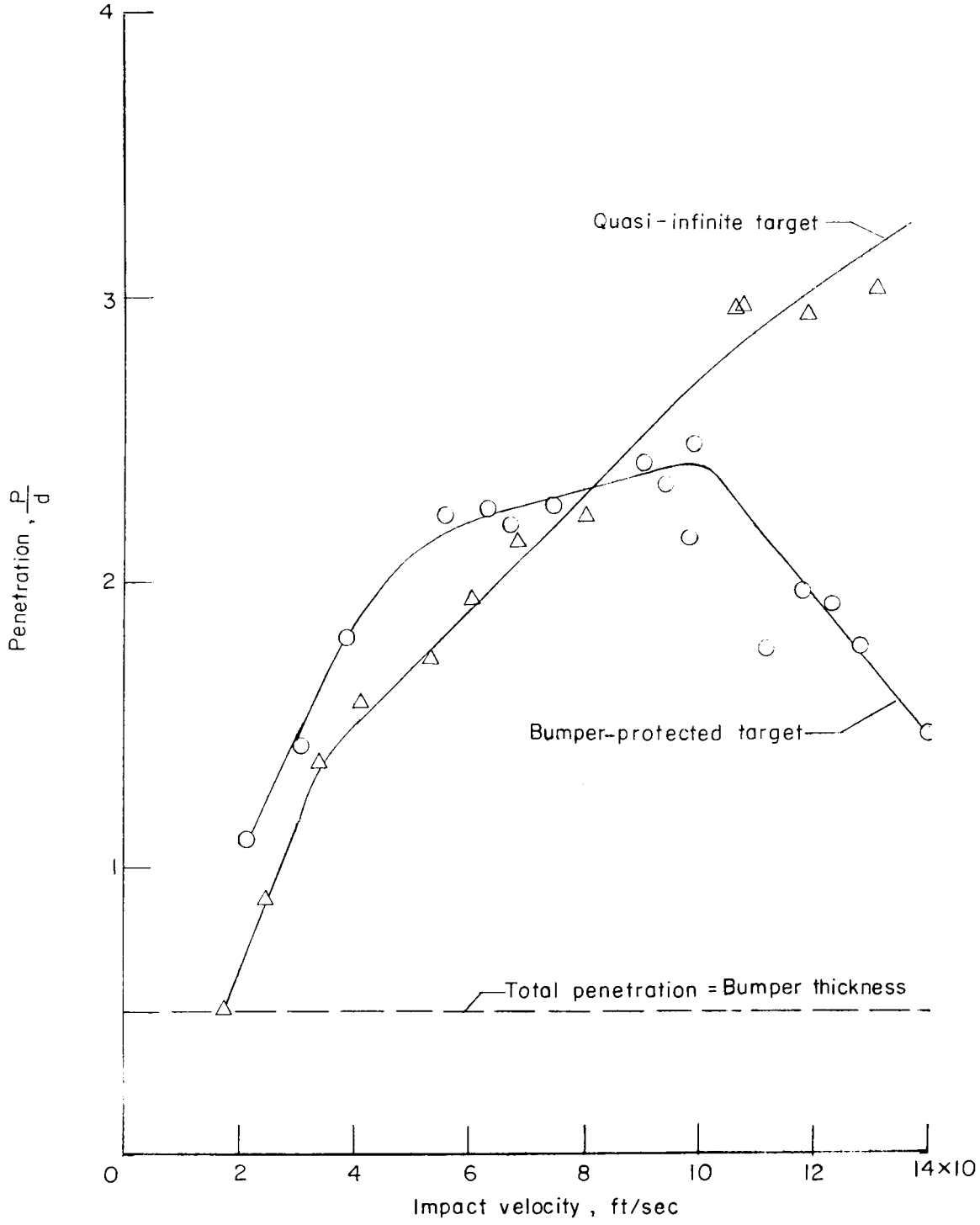

Figure 6.- Variation of total penetration with impact velocity in bumper-protected target. Bumpers were 0.031-inch-thick 2024-T3 aluminum alloy at a standoff of 2 inches; main walls were 1-inch-thick 2024-T4 aluminum alloy; projectiles were 0.062-inch-diameter copper spheres.

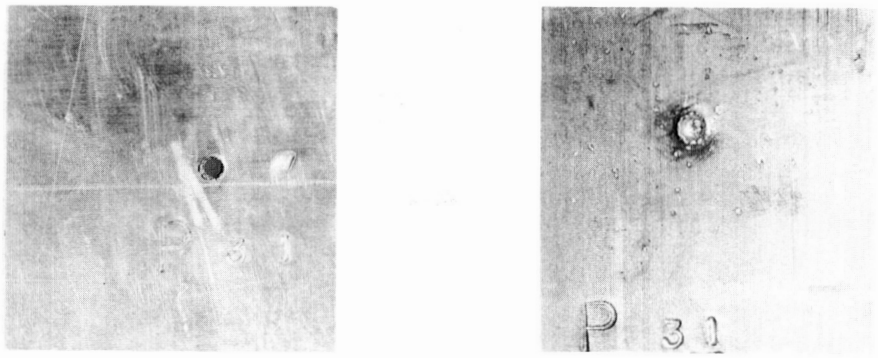

Bumper Main wall

(a) Impact velocity = 6,350 ft/sec.

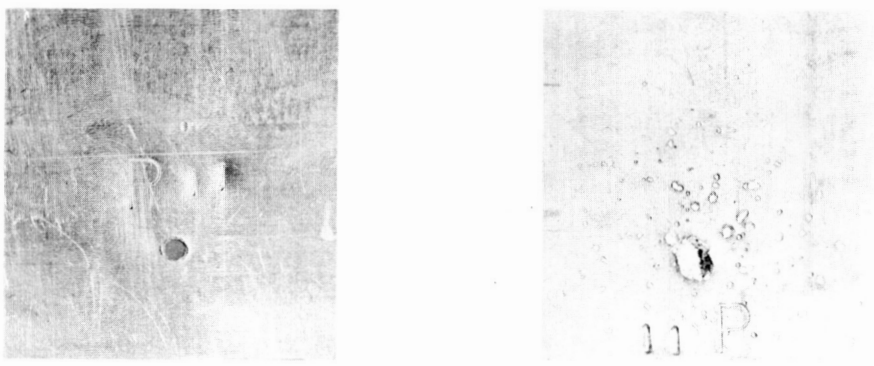

Bumper Main wall

(b) Impact velocity = 9,950 ft/sec.

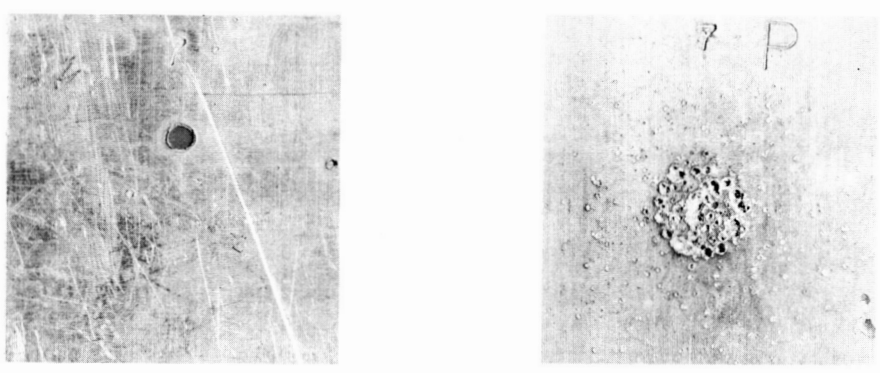

Bumper Main wall

(c) Impact velocity = 12,860 ft/sec.

L-63-59

Figure 7.- Damage to bumper-protected targets at various impact velocities. Bumpers were 0.031-inch-thick 2024-T3 aluminum alloy at a standoff of 2 inches; main walls were 1-inch-thick 2024-T4 aluminum alloy; projectiles were 0.062-inch-diameter copper spheres.

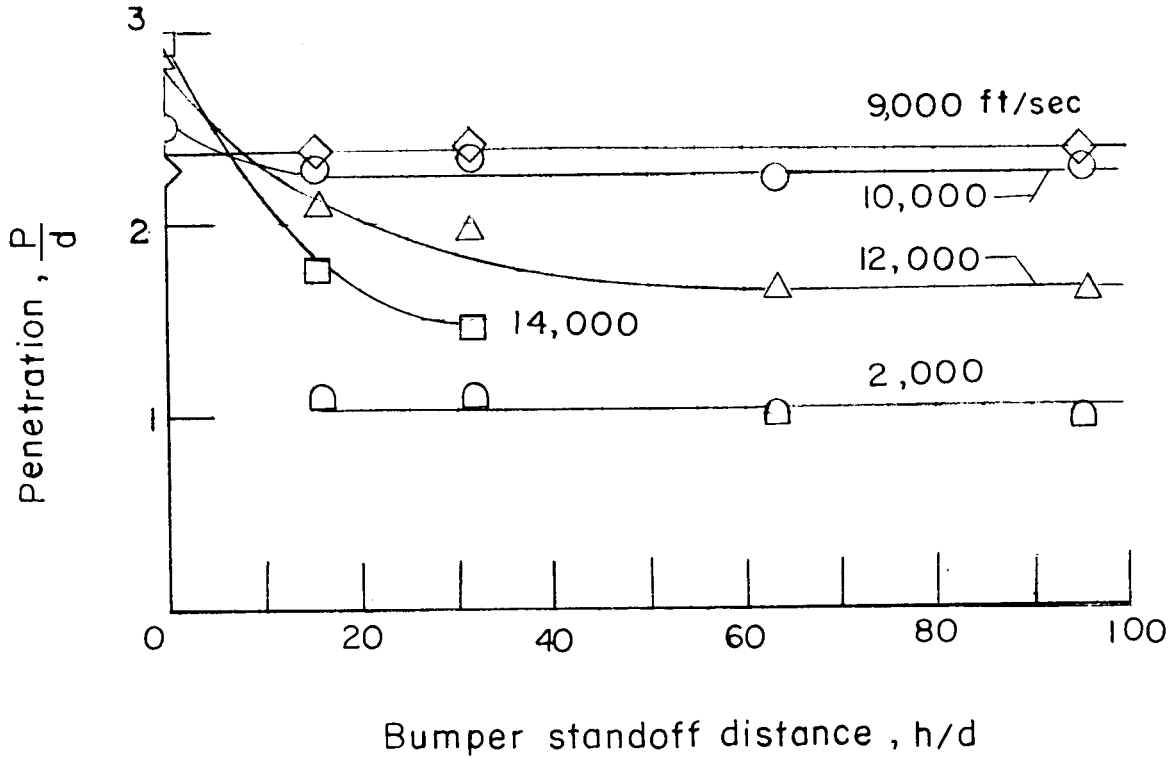

Figure 8.- Effect of bumper standoff distance on penetration at various impact velocities. Bumpers were 0.031-inch-thick 2024-T3 aluminum alloy; main walls were 1-inch-thick 2024-T4 aluminum alloy; projectiles were 0.062-inch-diameter copper spheres.

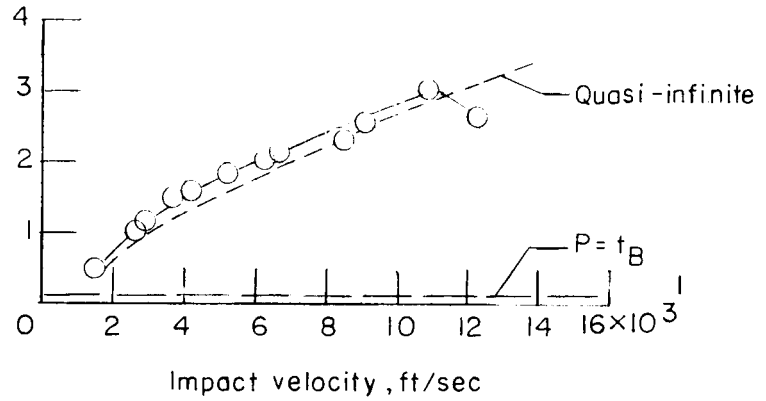

(a) $\frac{t_B}{d} = 0.16$.

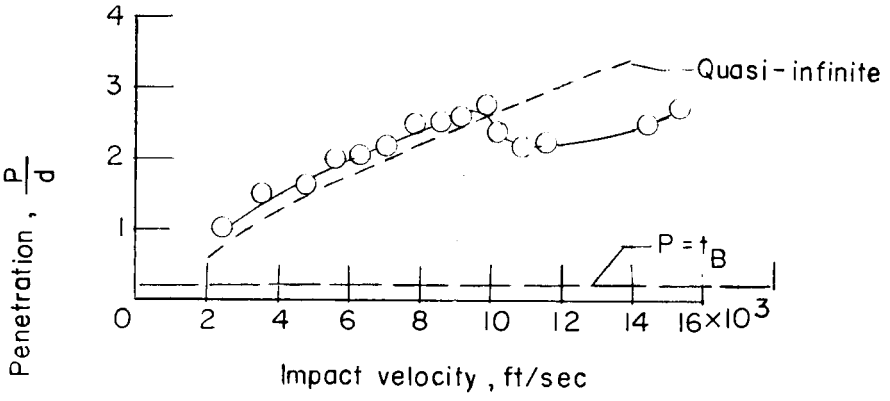

(b) $\frac{t_B}{d} = 0.25$

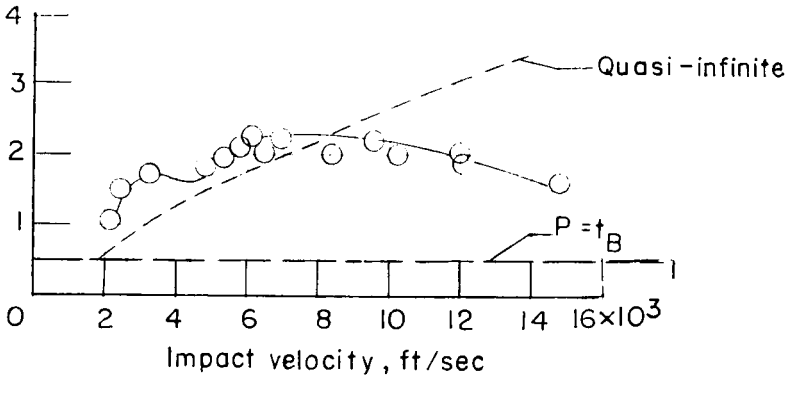

(c) $\frac{t_B}{d} = 0.5$.

Figure 9.- Effect of bumper thickness on the variation of total penetration with impact velocity. Bumpers were 2024-T3 aluminum alloy at a standoff of 1 inch; main walls were 1-inch-thick 2024-T4 aluminum alloy; projectiles were 0.062-inch-diameter copper spheres.

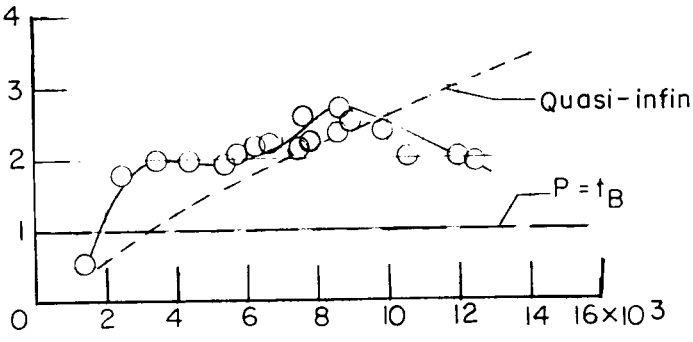

(d) $\frac{t_B}{d} = 1.0$.

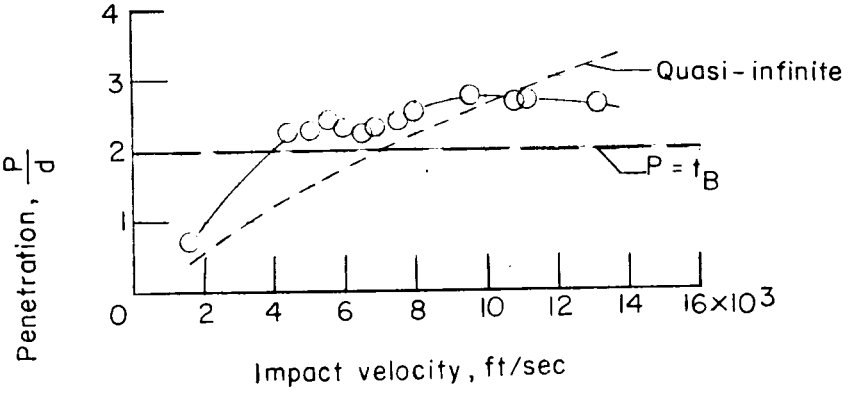

(e) $\frac{t_B}{d} = 2.0$.

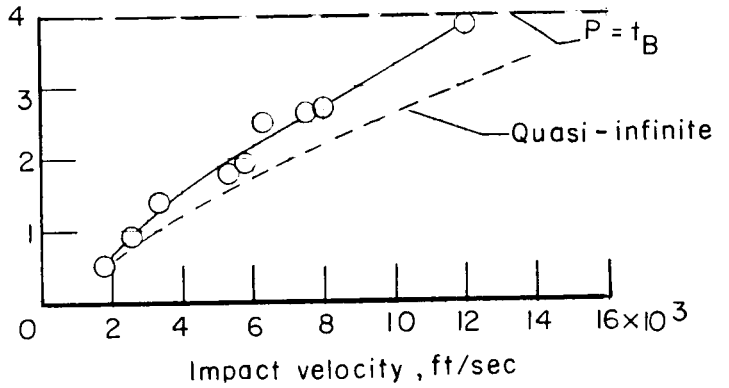

(f) $\frac{t_B}{d} = 4.0$.

Figure 9.- Concluded.

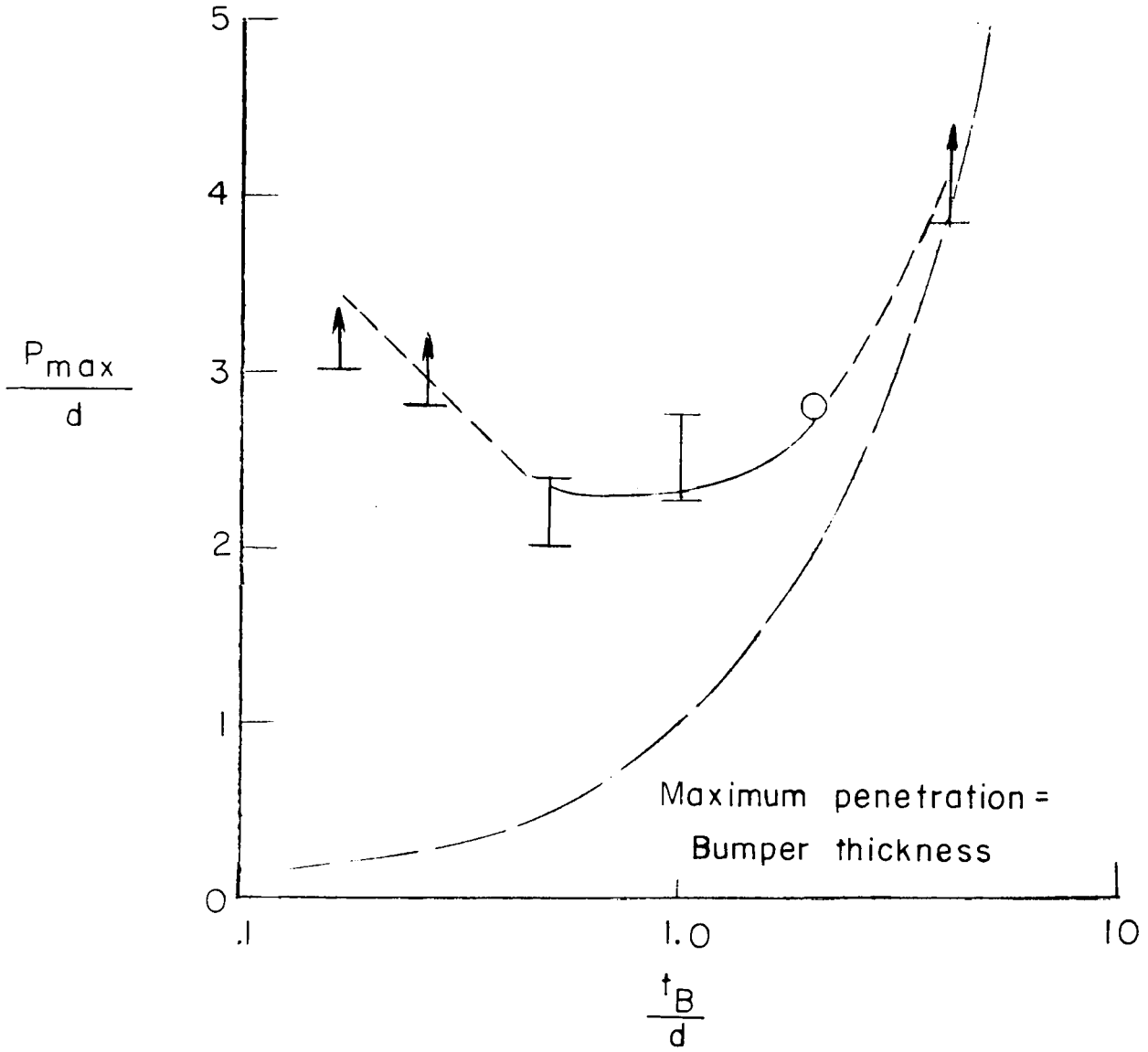

Figure 10.- Effect of bumper thickness on the maximum penetration. Bumpers were 2024-T3 aluminum alloy at a standoff greater than 8 projectile diameters; main walls were 1-inch-thick 2024-T4 aluminum alloy; projectiles were 0.062-inch-diameter copper spheres.

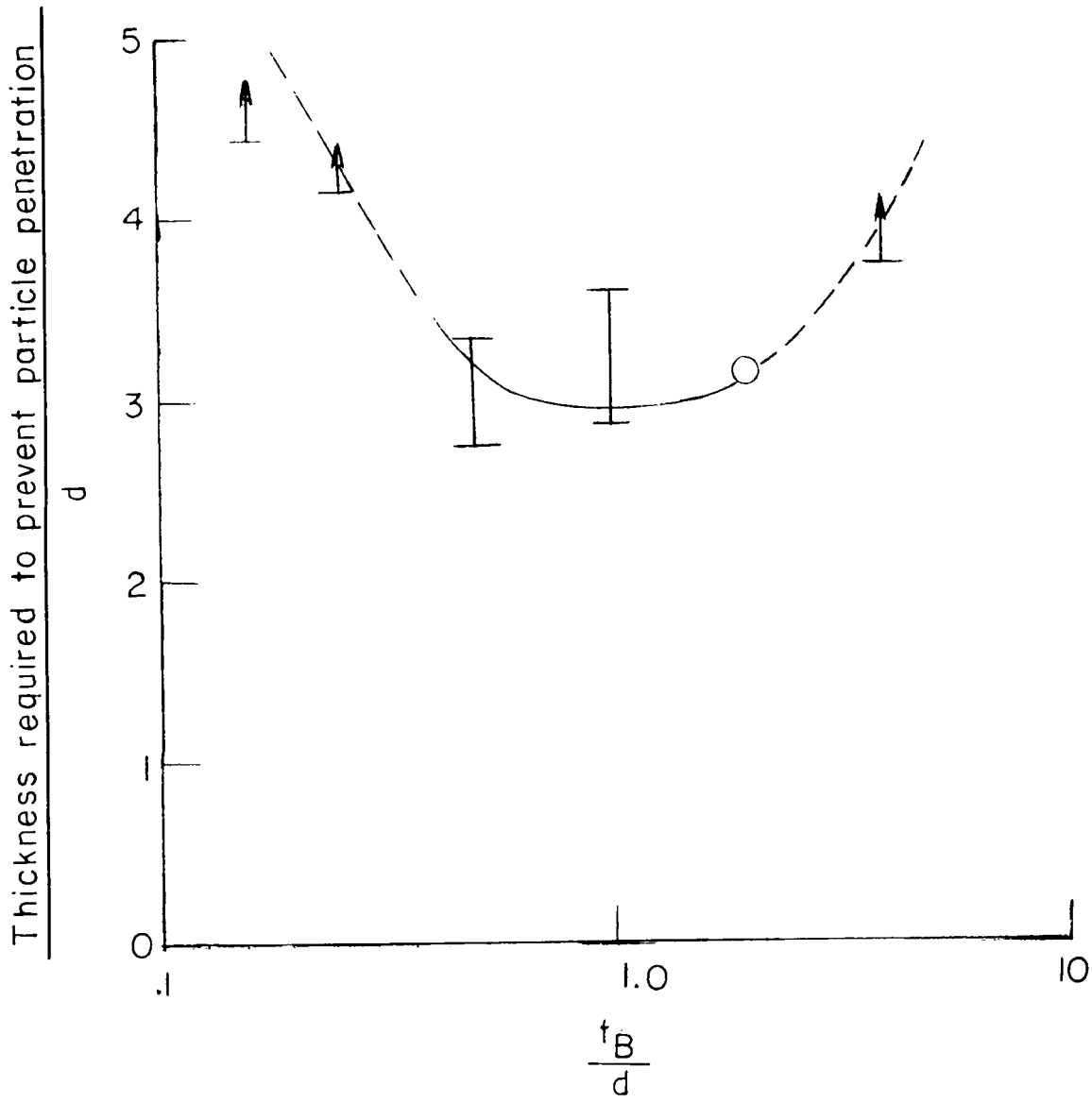

Figure 11.- Calculated effect of bumper thickness on minimum total thickness required to prevent complete penetration of projectiles at any impact velocity in the velocity range from 0 to 15,000 ft/sec. Bumpers were 2024-T3 aluminum alloy at a standoff greater than 8 projectile diameters; main walls were 1-inch-thick 2024-T4 aluminum alloy; projectiles were 0.062-inch-diameter copper spheres.